Colloid Polym Sci (2007) 285:1607–1615
DOI 10.1007/s00396-007-1735-4

ORIGINAL CONTRIBUTION

Preparation and characterization of multiresponsive polymer composite microspheres with core–shell structure

Jie Cai · Jia Guo · Minglei Ji · Wuli Yang · Changchun Wang · Shoukuan Fu

Received: 8 May 2007 / Revised: 25 June 2007 / Accepted: 26 June 2007 / Published online: 25 July 2007
© Springer-Verlag 2007

Abstract Fe_3O_4/SiO_2/poly (*N*-isopropylacrylamide-*co*-*N*, *N*-dimethylaminoethyl methacrylate) [P(NIPAM-*co*-DMA)] multiresponsive composite microspheres with core–shell structure were synthesized by template precipitation polymerization. First, the magnetite nanoparticles were coated with silica and then modified with 3-(trimethoxysilyl)-propyl methacrylate (MPS). Subsequently, the Fe_3O_4/SiO_2 particles grafted with MPS were used to seed the precipitation copolymerization of NIPAM and DMA. The composite microspheres with core–shell structure were superparamagnetic, pH-sensitive, and thermoresponsive. The swelling ratio $(D_{25\ °C,\ pH=3}/D_{50\ °C,\ pH=9})^3$ coupling of pH and temperature increased up to 21.2, which was much higher than that without comonomer DMA.

Keywords Polymer composite microspheres · Core–shell · Multiresponsive

Introduction

Stimuli-responsive polymer microspheres have attracted long-standing interest in the past decade due to their importantly reversible changes in their physical properties in response to various environmental stimuli such as temperature, pH, ionic strength, electrical field, magnetic force, mechanical stress, light, and so on [1–6]. Accordingly, these microspheres are widely used in both biomedical and biotechnology fields, such as drug delivery systems, specific molecular recognition, biosensors, affinity separations, and cell immobilizations, etc. [7]. Among stimuli-responsive polymer microspheres, thermoresponsive polymer microspheres, particularly those based on poly (*N*-isopropylacrylamide) (PNIPAM), have attracted much attention and were intensively investigated because PNIPAM exhibits a coil-globule transition upon exterior temperature changes [8, 9]. Since the report by Pelton in 1986 [1], PNIPAM microgels have been utilized in many fields, such as supporting material for biomedical testing [10], sorbent for proteins and active enzymes [11–14], and temperature-triggered drug or chemical release systems [15, 16].

More recently, with the development of stimuli-responsive polymers and their wide utility in a great many fields [17], different responses have been integrated into one composite microsphere by various ways so that the synthesized composite materials display multiform changes with the aid of external stimulus. Also, in the case of thermoresponsive polymers, more and more work has been extended to combine both temperature and other responsiveness into one single entity of multiplexed bioapplications [18, 19]. For example, Sauzedde et al. have reported that dual-responsive microspheres with temperature and magnetic responses could be prepared by physical adsorption of magnetite (iron oxide) nanoparticles onto PS-PNIPAM core–shell microspheres [20, 21]. Lyon et al. pursued the dual-responsive copolymer with pH/temperature stimuli-driven volume phase transitions, among which the most noted were related to the poly (NIPAM/AA) core–shell microgels [22–24]. They focused on the research concerning the different behavior influence of dual-responsive cores or dual-responsive shells toward the composite. Other pH-/thermo-responsive polymer microsphere investigations also include the NIPAM-*co*-vinylacetic acid microgels [25], NIPAM-*co*-methacrylic acid nanopar-

J. Cai · J. Guo · M. Ji · W. Yang (✉) · C. Wang · S. Fu
Key Laboratory of Molecular Engineering of Polymers (Minister of Education) and Department of Macromolecular Science, Fudan University,
Shanghai, China 200433
e-mail: wlyang@fudan.edu.cn

ticles [26], or NIPAM-*co*-*N*,*N*-dimethylaminoethyl methacrylate (DMA) microgel latexes [27].

In our previous works, the dual-responsive microspheres with one magnetic core and well-defined PNIPAM shell have been prepared by precipitation polymerization in the presence of modified magnetic silica templates [28, 29]. However, PNIPAM shells of tens of nanometers limited the swelling/deswelling ratios, leading to low efficiency of loading target molecules. On the basis of this consideration, other functional monomers were introduced to be copolymerized with NIPAM monomers for relatively larger volume change than the single thermoresponsive polymer [24, 26]. It has been reported that pH/temperature dual-responsive microgel with various structures exhibited different behaviors, especially in significantly changing particle volume under certain conditions. Triresponsive microspheres with pH-/temperature-responsive shells and magnetic cores, which were simultaneously introduced into one system, were developed in this work. Briefly, the stepwise core–shell functionalizations firstly began with functionalization of the Fe_3O_4/SiO_2 cores, which were treated to get the corresponding response to magnetism in favor of separation. Secondly, the multifunctional shell in response to temperature and pH was synthesized via precipitation polymerization onto the core by the copolymerization of NIPAM and DMA.

Experimental section

Materials

Ferric chloride hexahydrate ($FeCl_3 \cdot 6H_2O$, 98%, ACROS ORGANICS) and Ferrous chloride tetrahydrate ($FeCl_2 \cdot 4H_2O$, 99%, Fluka) were adopted. NIPAM (97%, Aldrich) and *N*,*N*′-methylenebis(acrylamide) (MBA, 98%, Fluka) were purified from 60/40 hexane/toluene mixtures and methanol, respectively. Potassium sulfate (KPS, Aldrich) was recrystallized from a 50/50 acetone/water mixture. DMA (98.5%, Tokyo Kasei Kogyo) and *N*,*N*-diethylaminoethyl methacrylate (DEA, 98.5%, Tokyo Kasei Kogyo) were purified by passing them through a basic Al_2O_3 column and distillation under reduced pressure, and then they were stored blow 0 °C. Other reagents were of reagent grade and were used as received. Deionized water was used.

Synthesis of the multiresponsive composite microspheres

Synthesis of magnetic nanoparticles

Colloidal magnetic nanoparticles were prepared by the coprecipitation of Fe^{2+} and Fe^{3+} (molar ratio of 1:2) by treatment with an aqueous solution of sodium hydroxide (10 mol/L) [30]. The as-prepared Fe_3O_4 nanoparticle colloid was treated with nitric acid (2 M) for 5 min and then washed with water until the supernate was neutral. Then the Fe_3O_4 colloid was dispersed in trisodium citrate solution (0.3 M) and kept at 90 °C for 0.5 h to prepare stable magnetite nanoparticles via electrostatic interaction. The obtained iron oxide dispersion was stabilized in water and adjusted to 2.0 wt.% for further use.

Modification of the magnetite nanoparticles with silica and 3-(trimethoxysilyl)-propyl methacrylate

The synthesized magnetic nanoparticle dispersion (0.4 g) was diluted with water (20 mL), and then ethanol (80 mL) was added. After adding ammonia solution (2.0 mL, 25 wt.%), the tetraethyl orthosilicate precursor (4 mL) was added to the reaction dispersion when the temperature of dispersion rose to 40 °C. Under continuous stirring, the reaction was carried out at 40 °C for 12 h. The obtained silica particles were modified with 3-(trimethoxysilyl)-propyl methacrylate (MPS) (2 mL) by stirring the mixture for another 12 h at 40 °C. The products (Fe_3O_4/SiO_2 particle grafted with MPS) were collected by magnet and washed three times with ethanol and water.

Preparation of multiresponsive microspheres

In the polymerization procedure, 0.8 wt.% dispersion of the Fe_3O_4/SiO_2 particles grafted with MPS was used to seed the precipitation copolymerization of NIPAM (0.1 g) and DMA with different weight contents. MBA was used as the crosslinker and KPS (4 mg, 4 wt.% content of NIPAM) as an initiator. The detailed recipes of input are listed in Table 1. Some distilled water was added to keep the total volume of 25 mL. The reaction was carried out at 70 °C for 4 h. Finally, the crosslinked composite microspheres [Fe_3O_4/SiO_2/P(NIPAM-*co*-DMA)] were washed several times with distilled water and enriched with the help of a magnet.

Apparatus and characterization

Transmission electron microscopy (TEM) images were obtained on a Hitachi H-600 TEM. The samples for the measurements were prepared by placing the copper grids coated with carbon into the product dispersion and then drying at room temperature. The copper grids were stained with phosphate-tungstic acid.

The hydrodynamic diameter of the particles was determined by quasielastic light scattering (Malvern Autosizer 4700). All dispersions used for the measurements were adjusted to the desired pH with HCl (0.1 mol/L) and/or

Table 1 Recipe for the preparation of multiresponsive microspheres

Sample code	Fe_3O_4/SiO_2 dispersion (g)	NIPAM (mg)	DMA (mg)	MBA (mg)	KPS (mg)
NM2051	6.25	100	1	5	4
NM2052	6.25	100	1.5	5	4
NM2053	6.25	100	2	5	4
NM2054	6.25	100	3	5	4
NM2055	6.25	100	4	5	4
NM4051	3.125	100	1	5	4
NM4052	3.125	100	1.5	5	4
NM4053	3.125	100	2	5	4
NM4054	3.125	100	3	5	4
NM4055	3.125	100	4	5	4
NM2101	6.25	100	2	10	4
NM2050	6.25	100	0	5	4

The Fe_3O_4/SiO_2 content of the pre-prepared dispersion is about 0.8 wt.%

NaOH (0.1 mol/L). During the measurement, the sample was allowed to equilibrate at the proper temperature for 5 min before data collection.

Thermogravimetric analysis (TGA) of the core–shell microspheres was performed with a Pyrisis 1 TGA instrument. About 2 mg of the sample was placed into a platinum crucible with increasing temperature (10 °C/min) in a controlled, flowing N_2 atmosphere, and heated from 50 to 800 °C.

The zeta potential of polymer magnetic composite microspheres was measured on a Zeta Potential Analyzer (Brookhaven). For zeta potential measurements, the samples were diluted with HCl and NaOH solution, respectively, to the right pH value in advance and measured in the automatic mode, and all measurements were performed in triplicate.

Ultraviolet-visible (UV-vis) adsorption spectra were measured at room temperature on a Lambda 35 (Perkin-Elmer) UV-vis spectrophotometer. According to the corresponding comonomer/(Fe_3O_4/SiO_2) weight ratios, the comonomer was added into Fe_3O_4/SiO_2 particle suspension and the mixture was incubated for 2 h, then the dispersion was centrifugated and the supernate was taken for the UV-vis adsorption measurement. A vibrating-sample magnetometer (VSM, EG&G Princeton Applied Research VSM, Model 155) was used to study the magnetic properties of multifunctional microspheres at room temperature.

Atomic absorption spectra were measured on a Polarized Zeeman Atomic Absorption Spectrophotometer (Z-5000) at room temperature for the measurement of Fe_3O_4 content. Fe_3O_4/SiO_2 particles were dissolved with hydrofluoric acid (HF). The excess HF was removed by evaporation and pH of the dispersion was tuned by diluted HNO_3. The dispersion was diluted to some degree, which was suitable for the atomic absorption spectrophotometer.

Result and discussion

Preparation of multiresponsive microspheres

The iron oxide dispersion was obtained following the method used by Sauzedde et al. [30], which was based on the coprecipitation of $FeCl_2$ and $FeCl_3$. Then, the product was treated with an excess of trisodium citrate solution to obtain the stable magnetite nanoparticles. The magnetite nanoparticles were coated with silica (as shown in Fig. 1a) via Stöber process [31], in which silica was formed in situ through hydrolysis and then condensation of tetraethyl orthosilicate. The obtained particle surfaces could be modified with commercially available silane coupling agent, such as MPS and 3-(triethyloxysilyl)-ethlene. In this case, the sequence of components input and selection of the silane coupling agent was determined by the pre-experiment results.

The formed Fe_3O_4/SiO_2 particles were about 100 nm, as shown in Fig. 1a. We note that the morphology of silica-

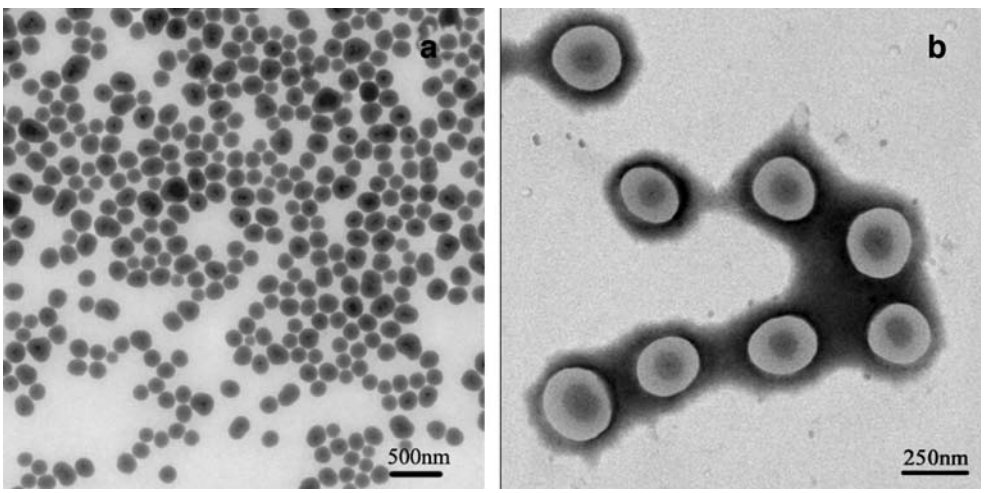

Fig. 1 TEM image of Fe_3O_4/SiO_2 particles (**a**), Fe_3O_4/SiO_2/P(NIPAM-*co*-DMA) composite microspheres for sample NM2053 [4 wt.% comonomer/(Fe_3O_4/SiO_2)] (**b**)

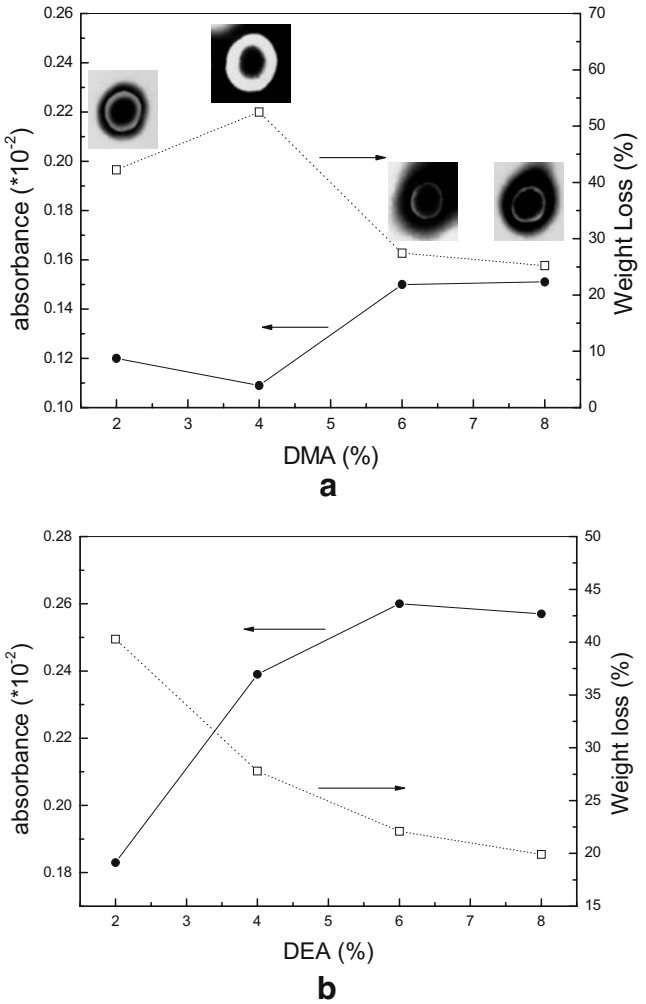

Fig. 2 The UV-vis absorbance of comonomers in the supernate (*circles*) (i.e., the comonomer which was not absorbed by Fe_3O_4/SiO_2 particles) and the polymer content (*squares*) in the composite microspheres which was characterized by the weight loss in TGA at different comonomer/(Fe_3O_4/SiO_2) weight ratios (2, 4, 6, and 8 wt.%): **a** DMA; **b** DEA

coated magnetic particles has well-defined structures, namely, all iron oxide nanoparticles were coated by the silica shells. Figure 1b shows the TEM image of the core-shelled, spherical polymer composite microspheres of Fe_3O_4/SiO_2/[P(NIPAM-*co*-DMA)] containing 4 wt.% co-monomer and 5 wt.% MBA, whose diameter was about 300±30 nm. The black dots, which were about 10 nm, were encapsulated in gray silica interlayer with a bright shell layer, which was a P (NIPAM-*co*-DMA) copolymer layer. Each P(NIPAM-*co*-DMA) shell contained one Fe_3O_4/SiO_2 core, as observed in Fig. 1b, and the microspheres with core–shell structure were well dispersed. Compared with the result of TEM for NM2053 [4 wt.% comonomer/(Fe_3O_4/SiO_2)], the diameter of the microspheres tested by DLS was 445 nm, and the parameter of the microspheres size distribution, polydispersity index ($PDI = \langle \mu_2 \rangle / \overline{\Gamma}^2$ [32]) was 0.077 when pH was 10 and temperature was 50 °C, which was larger than the diameter from TEM image (300±30 nm).

The aim of the present work was not only to prepare core–shell composite microspheres, but also to investigate the effect of the second monomer on the formation of polymer shells. Because the surface of the magnetic silica particles is acidic, it seemed that using a basic monomer would lead to a strong acid–base interaction [33]. In previous work, it was noted that the adsorption of other basic monomer such as pyridine onto silica substrates was well documented [34]. As a result, UV spectroscopy was used to monitor DMA depletion from aqueous dispersion in the presence of the Fe_3O_4/SiO_2 particles. In Fig. 2a, the absorbance of DMA in the supernate increased along with the increase of DMA to Fe_3O_4/SiO_2 particles, but the trend was nonlinear. Thus, it was possible that the comonomer DMA was partly dissolved in the aqueous phase and partly adsorbed at the surface of the Fe_3O_4/SiO_2 particles. According to the absorbance of DMA in the supernate, we can see that the adsorption of DMA by the Fe_3O_4/SiO_2 particles decreased along with the increase of DMA/(Fe_3O_4/SiO_2) weight ratio except the sample of 4 wt.% DMA/(Fe_3O_4/SiO_2). Correspondingly, the content of polymer layer shell, which was characterized by TGA in the collapsed state, reduced with the increase of DMA dissolved in aqueous dispersion except the case of 4 wt.% DMA/(Fe_3O_4/SiO_2). This was why the introduction of DMA monomer led to the formation of more precursors and promoted the colloidal stabilization of the nucleated particles via the electrostatic interaction; thus, the content of DMA that was initially dissolved in aqueous dispersion was greater, and the hydrophilic property that the DMA-rich copolymer possessed was greater, which inhibited the precipitation of P(NIPAM-*co*-DMA) onto the Fe_3O_4/SiO_2 particle surface, resulting in the formation of the thinner polymer shells. To confirm this hypothesis, DEA, another basic monomer, was chosen to conduct the same experiments, and the same trend was observed in Fig. 2b. In the case of 4 wt.% DMA/(Fe_3O_4/SiO_2), the thickest shells were obtained, but the reason for this was still less clear. We may need other related experiments to explain the phenomena.

As shown in Fig. 3a, the hydrodynamic diameter (PDI was around 0.1) increased to a maximum and then decreased with the increase of DMA. The result showed that the higher DMA content was, the bigger the particle size change was when pH was adjusted between 3 and 9. The hydrodynamic diameters of microspheres in collapsed state were obtained when temperature was 50 °C and pH was 9, as shown in Fig. 3b. The hydrodynamic diameter of microspheres changed with the variation of DMA amount, and the trend of the change was similar to the result of TGA and TEM (Fig. 2a). Because the Fe_3O_4/SiO_2 particles were well-defined uniform, the shell thickness changed as the

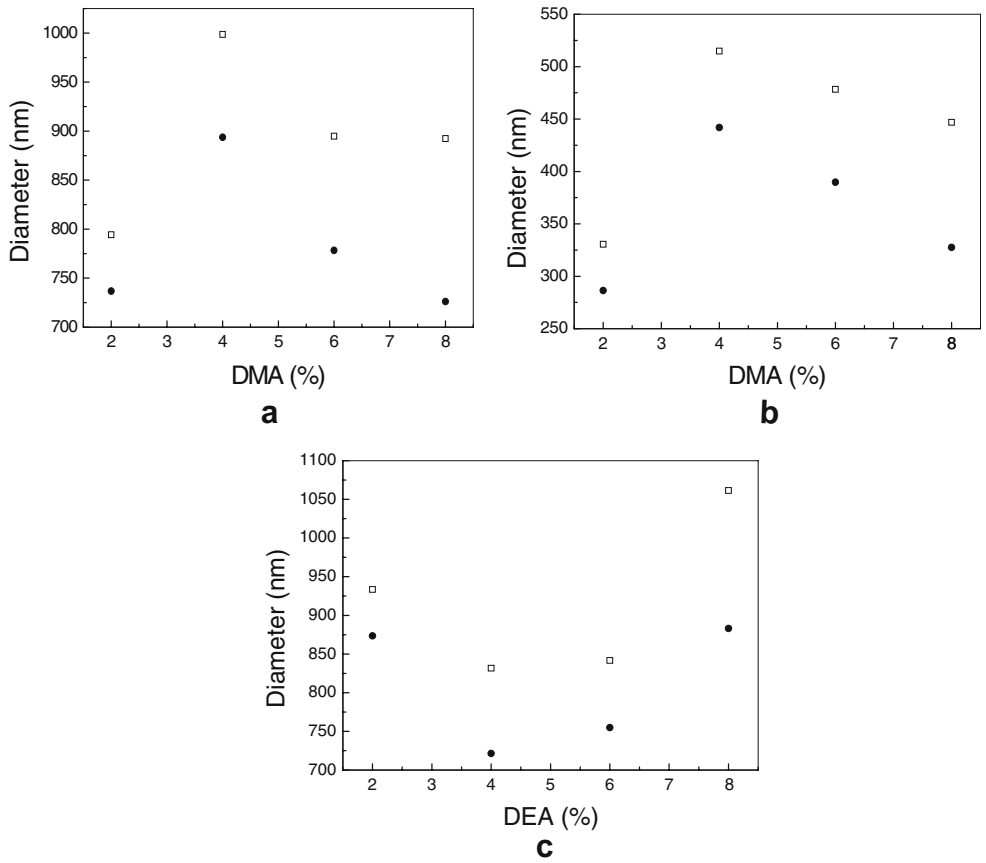

Fig. 3 The hydrodynamic diameter of the composite microspheres as a function of comonomer/(Fe_3O_4/SiO_2) weight ratio under pH=3 (*squares*) and pH=9 (*circles*): **a** DMA system, at room temperature; **b** DMA system, T=50 °C; **c** DEA system, at room temperature

hydrodynamic diameter of microspheres did. In the case of DEA (Fig. 3c), the trend was more clear. On the basis of the above-mentioned possibility, due to the adsorption amount of the basic monomer, the Fe_3O_4/SiO_2 particles stabilized by the negative charges were possibly adhered to each other because of a weakened electrostatic interaction. So the multiple Fe_3O_4/SiO_2 cores may be coated with the copolymers, leading to the big size in aqueous dispersion, and the TEM images (Fig. 4) also confirmed the different morphologies with multiple cores. When the amount of DEA was increased, the system of microspheres was not stable and the precipitates occurred in the dispersion. Additionally, it can be seen from Fig. 3a, c that the hydrodynamic diameter at pH 3 was larger than that at pH 9. This was a consequence of amino groups gaining protons under acidic condition and releasing them under basic condition. At pH 3, the microspheres were positively charged, and the electrostatic interaction between the chains in particles made the size of the particles increase. Consequently, the microspheres did indeed possess the pH response.

Aqueous microelectophoresis measurements were carried out on two microspheres at different pH values of the dispersion to describe the behavior of pH response (Fig. 5). As expected, the zeta potential decreased gradually when the pH of dispersion increased, and the zeta potential curve suggested that the isoelectric points of the two microspheres were around pH 7. The zeta potential of the sample which contained more DMA (NM2055) was higher than the other (NM2051) at lower pH, and it illuminated that the DMA content had an effect on the zeta potential (pH response). The microspheres exhibited positive zeta potential before pH of dispersion reached the isoelectric point, as it was evaluated, as PDMA was quaternized in acid condition (below the isoelectric point).

The magnetic property of these microspheres was analyzed by VSM. The saturation magnetization of the synthetic composite microspheres was found to be equal to 1.66 emu/g at 305 K (Fig. 6). In addition, when the magnetic field intensity decreased to zero, the magnetization decreased from the plateau value and closed to zero, suggesting that the coercive force was very low. The obvious superparamagnetic property can be observed for the nanoparticles from the classic "S" shape magnetite curve, and this property can prevent the polymer magnetic composite microspheres from aggregation and enable them to redisperse rapidly when the magnetic field was removed.

Atomic absorption spectra was adopted to test the content of the magnetite nanoparticles. The Fe_3O_4/SiO_2 particles

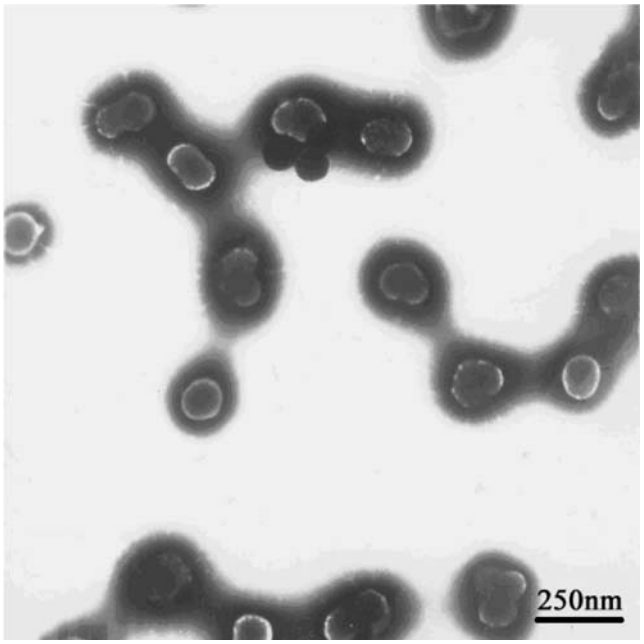

Fig. 4 TEM image of Fe_3O_4/SiO_2/P(NIPAM-*co*-DEA) composite microspheres [8 wt.% comonomer/(Fe_3O_4/SiO_2)]

(0.20 g) were dissolved with HF. The dispersion was diluted for the atomic absorption spectrophototer measurement, and the content of ferric and ferrous was 6.33 mg; then we calculated that the weight of Fe_3O_4 was 8.74 mg. The copolymer shell content was about 44.2%, which tested by TGA. Thus, the content of the magnetite nanoparticles was 2.44% in the polymer composite microspheres.

Temperature and pH responsive of the microspheres

As shown in Fig. 7, the hydrodynamic diameter decreased gradually with increased pH, which was attributed to the

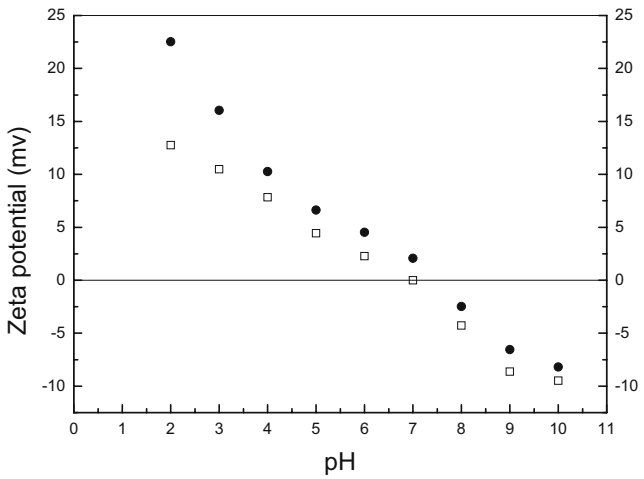

Fig. 5 The zeta potentials as a function of pH of samples NM2051 [2 wt.% DMA/(Fe_3O_4/SiO_2)] (*squares*) and NM2055 [8 wt.% DMA/(Fe_3O_4/SiO_2)] (*circles*)

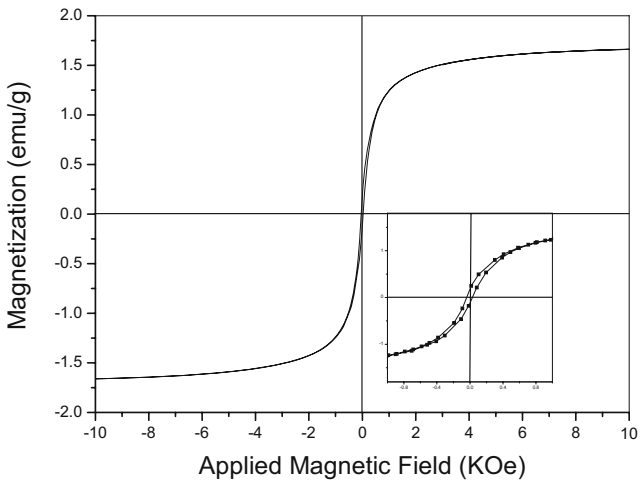

Fig. 6 Magnetization vs applied magnetic field for Fe_3O_4/SiO_2/P(NIPAM-*co*-DMA) microspheres at 305 K. The *inset* is a magnified view of the magnetization curves at low applied fields

repulsion between the protonated groups. When pH was around the isoelectric point (pH ~6–8), the hydrodynamic diameter of the microspheres changed a little because the charge decreased and the steric stabilization may have operated mainly. It was known that the pKa was also affected by the length of the polymer chain. Because of the existence of the crosslinker, the length of the polymer chains was different in the network; the pKas of different polymer chains were also different from each other to a certain extent. Because of the inhomogeneity of the length of polymer chains, the transition range of size became broader with the decrease of pH, then there was no sharp turning point. Thus, with the decrease of pH, we only observed that the size of microspheres increased gradually. The same result was also obtained from sample NM2055, which had a more extensive response to the pH change (as shown in Fig. 7).

Herein, as shown in Fig. 5, the variation in the zeta potential of mutiresponsive microspheres displayed a similar trend as polyampholyte microgels, which had zwitterionic properties [35]. However, in fact, the hydrodynamic size of microspheres decreased with the increase of pH, and then kept constant at high pH. In contrast to a previous report [35], the polymer shells around the magnetic silica particles did not show the zwitterionic properties because the formation of cross-linked shells was based on the copolymerizaion of NIPAM and DMA (or DEA) monomers. As a result, the swelling change was ascribed to the protonated PDMA (or PDEA) chains at low pH, whereas, at high pH, the size should keep constant due to the polymer shells being uncharged. On the other hand, the silica layers sandwiched by the polymer shells and magnetite nanoparticles should exhibit electronegative property owing to the ionization of Si–OH at pH>7. Thus,

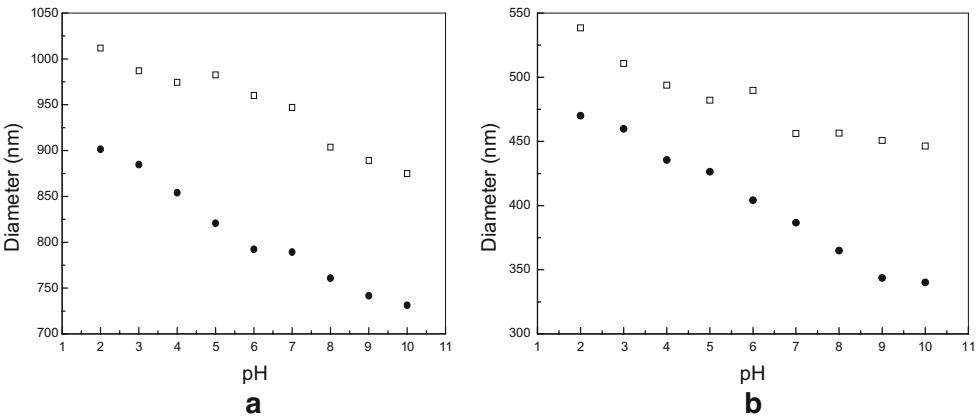

Fig. 7 Hydrodynamic diameter of the multiresponsive microspheres as a function of pH of the sample NM2053 [4 wt.%, DMA/(Fe_3O_4/SiO_2)] (*squares*) and the sample NM2055 [8 wt.% DMA/(Fe_3O_4/SiO_2)] (circles) at respective temperature: **a** T=25 °C; **b** T=50 °C

the composite microspheres showed the negative zeta potential as shown in Fig. 5 at pH>7, while the PDMA (or PDEA) chains have been deprotonated and became neutral. So, it was just observed that the hydrodynamic size of microspheres decreased with the increase of pH and kept constant at the high pH, as shown in Fig. 7.

The thermosensitive volume phase transition was strongly dependent on the copolymer compositions [26]. Figure 8 exhibited the hydrodynamic diameter as a function of temperature for Fe_3O_4/SiO_2/P(NIPAM-*co*-DMA) microspheres with two different DMA contents at different pH values. Two features should be noted. First, the critical volume phase transition temperature (T_{VPT}) slightly increased with the increase of DMA content. T_{VPT} depended on the balance of hydrophobic/hydrophilic interactions between the polymer chains and water. In the past, many researchers focused on checking the hydrophobic/hydrophilic effect on T_{VPT}. The hydrophobic interaction lowered T_{VPT} and the hydrophilic interaction raised T_{VPT} [36, 37]. It is known that the lower critical solution temperature of PNIPAM is about 32 °C [38]. The trend of Fig. 8a suggests that T_{VPT} of NM2053 was in the range of 36–40 °C, which was around the temperature of a human being. So the multiresponsive microspheres prepared by this way would be used as a carrier for anticancer drug delivery [39]. Here, incorporation of the monomer DMA resulted in increasing T_{VPT} because PDMA chains were more hydrophilic than PNIPAM chains. Second, the transition became broader with increasing DMA content, which is shown in Fig. 8b, with a more gently diameter decreasing compared with that of Fig. 8a. The broader transition range might be attributed to the inhomogeneity of PNIPAM chains in the network. It is known that the polymer chains with different lengths undergo phase transitions at different temperatures. For the random copolymerization of NIPAM and DMA, the PNIPAM chains inside the network had a broad molecular weight (chain length) distribution. Increasing DMA content, the molecular weight (chain length) distribution of the thermoresponsive PNIPAM chains that had been copolymerized randomly were broadened. The higher the DMA/NIPAM molar ratio in the feed composition, the larger the PNIPAM chain length difference, and then the T_{VPT} range was broadened. As shown in the last column of Table 2, the swelling ratio defined as $(D_{25\ °C,\ pH=3}/D_{50\ °C,\ pH=9})^3$ was a coupling of pH and temperature variables. The results suggest that more controllable multiresponsive microspheres could be prepared by adjusting the DMA content. Compared with NM2050 (the swelling ratio was 8.4 and without DMA incorporation), the volume of the samples with DMA can change in a much larger scale, and the

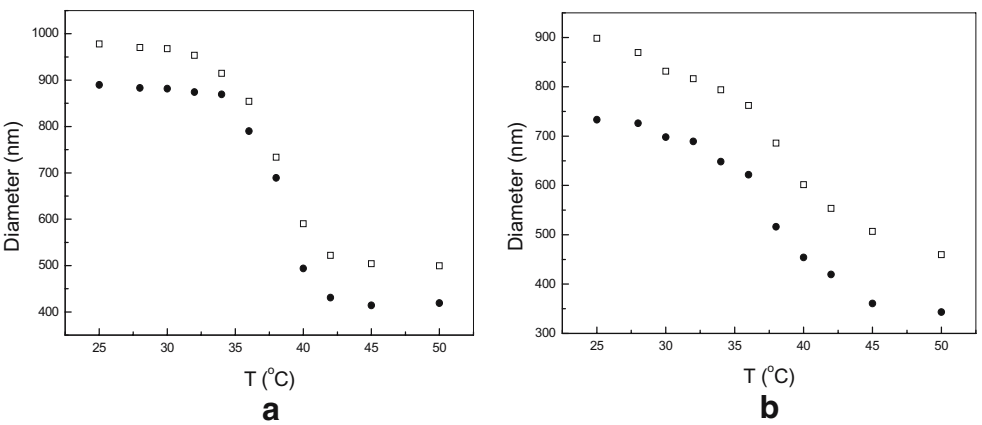

Fig. 8 Hydrodynamic diameter of the multiresponsive microspheres as a function of temperature at pH=3 (*squares*) and pH=9 (*circles*): **a** sample NM2053 [4 wt.% DMA/(Fe_3O_4/SiO_2)]; **b** sample NM2055 [8 wt.% DMA/ (Fe_3O_4/SiO_2)]

Table 2 Influence of pH and temperature on the hydrodynamic diameter of multiresponsive microspheres and the swelling ratio

Sample code	Hydrodynamic diameter (nm)		Swelling ratio ($D_{25\ °C,pH=3}/D_{50\ °C,pH=9})^3$
	Diameter (25 °C, pH=3)	Diameter (50 °C, pH=9)	
NM2050	710	350	8.4
NM2051	795	285	21.2
NM2052	800	310	17.5
NM2053	1000	440	11.5
NM2054	900	390	12.1
NM2055	890	330	20.2

largest swelling ratio can reach 21.2 [2 wt.% DMA/(Fe_3O_4/SiO_2)], which was larger than other PNIPAM microsphere swelling ratios obtained by some researchers [24, 25, 27]. To obtain such microspheres with variable volume change to the external stimuli was one of our purposes.

Other influence factors

Slightly crosslinked systems are typically swollen more than highly crosslinked systems [22, 23]. As shown in Fig. 9, the swelling ratio (the ratio of the swelling volume to the deswelling volume under the guidance of the environment stimuli), defined as $(D_{25\ °C,\ pH=3}/D_{50\ °C,\ pH=9})^3$ with 10 wt.% MBA content, was approximately 8.2, which was lower compared with NM2053 (11.5) with 5 wt.% MBA content shown in Fig. 8a. The swelling ratio depended on the number of chains with different lengths, and the average number of chains that will be perturbed will differ according to the initial crosslinker concentration. The microspheres with lower crosslinker content had a longer average chain length; accordingly, the transition range of the hydrodynamic diameter was narrower than the particles with higher crosslinker content [22, 23]. This kind of microsphere could be widely used in in vitro enrichment and temperature-controlled releases for the target biomolecules [8, 17].

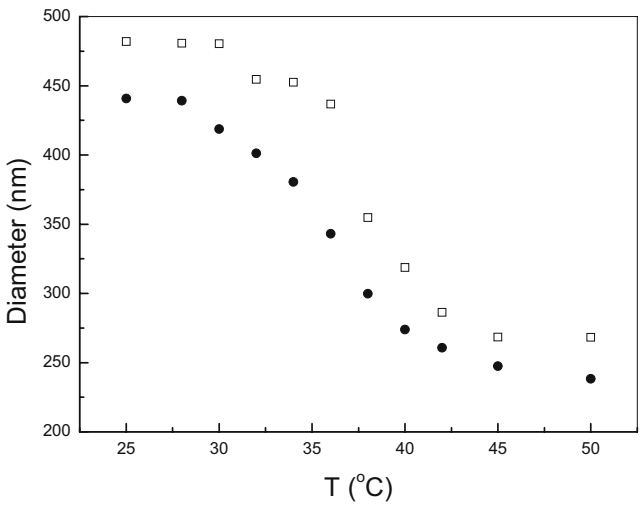

Fig. 9 Hydrodynamic diameter of the sample NM2101 (10 wt.% MBA content) as a function of temperature at pH=3 (*squares*) and pH=9 (*circles*)

As the thermoresponsive monomer, NIPAM was very popular in researches, but the selection of the pH-responsive monomer had taken a lot of time, such as 4-VP, DMA, and DEA, which all belonged to polybases. When 4-VP was used as the pH-responsive monomer, the obtained microspheres did not possess of the perfect core–shell structure and the shell was thinner than that with DMA, and the same deficiency of structure also appeared in some researches [40, 41]. When DEA was adopted as the monomer, the obtained microspheres had a relatively nice core–shell structure, as the ones prepared with DMA, but the diameter change with pH was smaller than that prepared with DMA (Fig. 3), so our investigation focused on the study of the behavior of the multiresponsive microspheres with the incorporation of DMA.

Conclusions

Fe_3O_4/SiO_2/P (NIPAM-*co*-DMA) multiresponsive composite microspheres with core–shell structure were synthesized in water by precipitation polymerization. The magnetite nanoparticles endowed the superparamagnetic property for the composite microspheres. The present work investigated the effect of the second monomer on the formation of polymer layer shell and also illustrated that the more DMA was dissolved in aqueous dispersion initially, the more hydrophilic the copolymer was, resulting in the formation of the thinner polymer shell. The hydrodynamic diameter of Fe_3O_4/SiO_2/P(NIPAM-*co*-DMA) microspheres decreased gradually when pH increased and underwent a volume phase transition with temperature, which was strongly dependent on the copolymer compositions: (1) the T_{VPT} increased with increasing DMA content and (2) the transition became broader with increasing DMA content. The swelling ratio $(D_{25\ °C,pH=3}/D_{50\ °C,pH=9})^3$ coupling of pH and temperature variables was much higher than that without DMA and reached 21.2 [2 wt.% DMA/(Fe_3O_4/SiO_2)]. Thus, a new approach was developed to prepare the responsive microspheres, and the combination of several desired functions in a single object was realized.

Acknowledgements We are grateful for the financial support of the Natural Science Foundation of China (No.50403011, 50525310) and the Science and Technology Commission of the Shanghai Municipality (05QMX1404 and 05DJ14005).

References

1. Pelton RH, Chibante P (1986) Colloids Surf 20:247
2. Sauer M, Streich D, Meier W (2001) Adv Mater 13:1649
3. Zhang JG, Xu SQ, Kumacheva E (2004) J Am Chem Soc 126:7908
4. Ibarz G, Dahne L, Donath E, Mohwald H (2001) Adv Mater 13:1324
5. Neyret S, Vincent B (1997) Polymer 38:6129
6. Wu XY, Zhang Q, Arshady R (2003) In: Arshady R (ed) Introduction to polymeric biomaterials, PBM, vol. 1. Citus Books, London, pp 157–231
7. Nayak S, Lyon LA (2005) Angew Chem Int Ed Engl 44:7686
8. Kawaguchi H (2000) Prog Polym Sci 25:1171
9. Berndt I, Pedersen JS, Richtering W (2006) Angew Chem Int Ed Engl 45:1737
10. Delair T, Meunier F, Elaissari A, Charles MH, Pichot C (1999) Colloids Surf A Physicochem Eng Asp 153:341
11. Achiha K, Ojima R, Kasuya Y, Fujimoto K, Kawaguchi H (1995) Polym Adv Technol 6:534
12. Kawaguchi H, Fujimoto K, Mizuhara Y (1992) Colloid Polym Sci 270:53
13. Fujimoto K, Mizuhara Y, Tamura N, Kawaguchi HJ (1993) Intell Mater Syst Struct 4:184
14. Yasui M, Shiroya T, Fujimoto K, Kawaguchi H (1997) Colloids Surf B Biointerfaces 8:311
15. Snowden MJ, Vincent B (1992) J Chem Soc Chem Commun 16:1103
16. Kato T, Fujimoto K, Kawaguchi H (1994) Polym Gels Netw 2:307
17. Suzuki D, Kawaguchi H (2006) Colloid Polym Sci 284:1471
18. Schmidt AM (2007) Colloid Polym Sci 285:953
19. Wong JE, Gaharwar AK, Müller-Schulte D, Bahadur D, Richtering W (2007) J Magn Magn Mater 311:219
20. Sauzedde F, Elaissari A, Pichot C (1999) Colloid Polym Sci 277:846
21. Sauzedde F, Elaissari A, Pichot C (1999) Colloid Polym Sci 277:1041
22. Jones CD, Lyon LA (2003) Langmuir 19:4544
23. Jones CD, Lyon LA (2003) Macromolecules 36:1988
24. Jones CD, Lyon LA (2000) Macromolecules 33:8301
25. Hoare T, Pelton R (2004) Macromolecules 37:2544
26. Zhou SQ, Chu B (1998) J Phys Chem B 102:1364
27. Zha LS, Hu JH, Wang CC, Fu SK, Elaissari A, Zhang Y (2002) Colloid Polym Sci 280:1116
28. Deng YH, Yang WL, Wang CC, Fu SK (2003) Adv Mater 15:1729
29. Guo J, Yang WL, Deng YH, Wang CC, Fu SK (2005) Small 1:737
30. Sauzedde F, Elaissari A, Pichot C (1999) Colloid Polym Sci 277:846
31. Stöber W, Fink A, Bohn E (1968) J Colloid Interface Sci 26:62
32. Chu B, Wang Z, Yu J (1991) Macromolecules 24:6832
33. Barthet C, Hickey AJ, Cairns DB, Armes SP (1999) Adv Mater 11:408
34. Percy MJ, Michailidou V, Armes SP (2003) Langmuir 19:2072
35. Das M, Kumacheva E (2006) Colloid Polym Sci 284:1073
36. Winnik FM (1990) Macromolecules 23:233
37. Feil H, Bae YH, Feijen J, Kim SW (1993) Macromolecules 26:2496
38. Schild HG (1992) Prog Polym Sci 17:163
39. Deng YH, Wang CC, Shen XZ, Yang WL, Jin L, Gao H, Fu SK (2005) Chem Eur J 11:6006
40. Percy MJ, Barthet C, Lobb JC, Khan MA, Lascelles SF, Vamvakaki M, Armes SP (2000) Langmuir 16:6913
41. Percy MJ, Michailidou V, Armes SP (2003) Langmuir 19:2072